An Alternative Approach for Pattern Detection Applied to Materials Characterization

Raul Queiroz Feitosa[1,3], Guilherme Mota[1], Sidnei Paciornik[2]

[1]Dept. of Electrical Engeneering ; [2]Dept. of Material Science
Catholic University of Rio de Janeiro
Rua Marquês de São Vicente, 225
22453-900, Rio de Janeiro
Brazil

[3]Dept. of Computer Engineering
State University of Rio de Janeiro
Rua São Francisco Xavier, 524
20550-013, Rio de Janeiro
Brazil

e-mail: raul@ele.puc-rio.br; guimota@ele.puc-rio.br; sidnei@dcmm.puc-rio.br

ABSTRACT

The problem of detecting specific patterns in images of materials obtained through High Resolution Transmission Electron Microscopy is addressed. A supervised classification method is proposed using an extension of Principal Component Analysis and a new a procedure for building the training set. Experiments on two different types of images indicate that the proposed method is superior to the conventional cross-correlation approach. Moreover, using the same number of components, the new dimensionality reduction approach shows a better performance than the standard PCA method.

Keywords: pattern recognition, dimensionality reduction, materials characterization

1. INTRODUCTION

The everyday properties of materials are strongly dependent on their microscopic organization. The characterization of this so-called "microstructure" is undertaken through a large number of techniques including optical microscopy and electron microscopy. The microstructure at atomic level can be analyzed through a specific technique called High Resolution Transmission Electron Microscopy (HRTEM). Electrons are accelerated and traverse a very thin specimen of the material, providing an image where bright and dark dots can be correlated to the positions of atomic columns in a crystalline sample.

Fig. 1 shows an HRTEM image of a small portion of a ceramic material, TiO_2. Two distinct regions can be seen at the top and bottom of the image. Both have the same geometric organization but are rotated in relation to each other. Each region is called a crystal (or grain) and is highly organized in a periodic fashion. The boundary between the two regions, called a grain boundary, is extremely important for the properties of the material. The presence of grain boundaries may have deleterious effects on the mechanical and electronic properties. A large portion of the research to improve the strength of materials uses HRTEM to image the grain boundaries at high magnification and analyze their structure.

The analysis many times aims at locating specific patterns of the image dots. Fig. 2 is an enlarged view of Figure 1, where two patterns of interest, the so-called structural units of the boundary, are highlighted. Once an operator has identified one or more of these patterns, it is desired to locate the occurrences of similar patterns along the whole boundary. This is a typical supervised pattern recognition procedure

Pattern recognition has been used before to semi-automatically locate structural units in HRTEM images of grain boundaries. In these works [Pacio96][Dahme94] the cross-correlation coefficient (CCC) was used as a measure of similarity between the whole image and a template unit chosen by the operator.

Fig. 3 shows the results of this procedure as reported in [Pacio96]. In this image, the pixel brightness maps the similarity between the original image and the left template marked in Fig 2. A similar image can be obtained for the other template.

The CCC image becomes easier to analyze if a threshold operator is applied, keeping only points of high CCC value. This is shown in Fig 2 where the peak CCC values for both templates are combined. The bright dots correspond to the location of the centers of the structural units.

Immediate consequence of this analysis is a

better visual interpretation of the image. It becomes clear that the boundary is composed of five plateaux, separated by steps. The structural units of both kinds appear only at the plateaux, in alternating positions. This is relevant information to the materials scientist and its consequences were explored in [Pacio96][Dahme94].

The application at hand has two important characteristics. First, there are few available examples to build a training set that characterizes properly the class of patterns to be detected. During the training phase the user must provide to the system some examples of regions enclosing a pattern of the boundary. However this is exactly the task that the automatic system ought to do for the user. So it is desirable that the training procedure requires as few examples as possible of the class to be detected. The approach presented in this paper minimizes the intervention of the user by requiring the indication of just one region containing the pattern to be detected.

Second, the patterns not belonging to the class to be detected are, on the contrary, abundant in the input image. The proposed method presents also a semi automatic procedure to collect many *non-boundary* examples with little user intervention.

The classic CCC based procedure does not take advantage of the second characteristic of this application. It is based on a single template that will represent the pattern to be located, without exploring the knowledge about the other patterns present in the image. As a matter of fact, the CCC method is very sensitive to the threshold value. A lower threshold value will lead to the acceptance of spurious patterns as structural units - false detections. A higher threshold, on the other hand, will lead to false rejections - true structural units that are not recognized.

The goal of this paper is therefore to propose a new method to detect structural units in

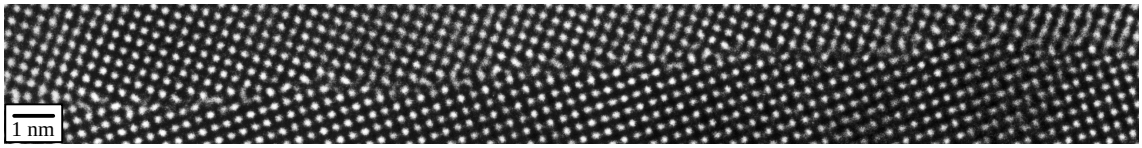

HRTEM image of a grain boundary in TiO_2. Note the top and bottom crystals that meet at a boundary
Figure 1

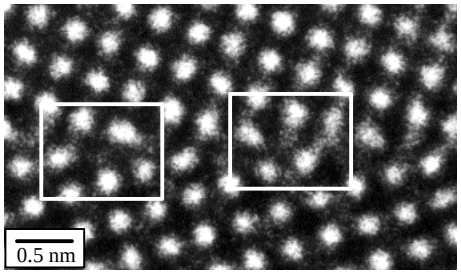

Enlarged portion of Fig.1 showing structural units of the boundary
Figure 2

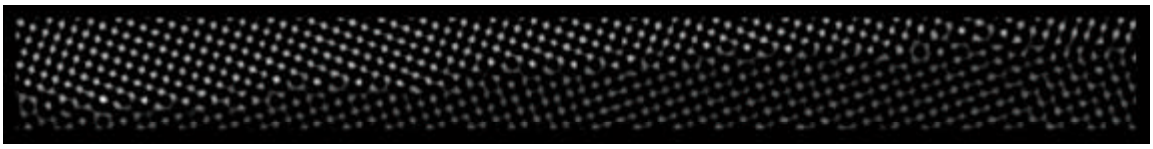

The cross-correlation image between the original image and the left template shown in Fig. 2
Figure 3

The location of structural units in the boundary of Fig 1, as determined by template-matching through cross-correlation (from [Pacio96]).
Figure 4

HRTEM images, having a better tradeoff between the number of false detections and false rejections than the conventional cross correlation technique. Besides providing a better solution to an important problem in the area of materials science, this approach has two important contributions that can be applied to other pattern recognition applications:

- a new technique for dimensionality reduction is developed by adapting Principal Component Analysis (PCA) to the problem of pattern detection, and
- a semi-automatic procedure to collect examples for the training sets which reduces user intervention to a minimum.

The next section describes the proposed detection system. Section 3 describes the procedure to collect training examples from the input image. Section 4 presents the experiments carried out to test the method and compares its performance with the results obtained by template matching through cross-correlation.

2. DESCRIPTION OF THE SYSTEM

The detector proposed in this work can be viewed as a non-linear neighborhood operation of the form:

$$c(x,y) = T[f(x,y)], \tag{1}$$

where $f(x,y)$ is the pixel intensity of the input gray level image at the coordinates (x,y), T is a non-linear operator defined in the rectangular neighborhood $w(x,y)$ of dimension a×b around the pixel at (x,y), and $c(x,y)$ is the class associated to the image window by the operator. Thus the patterns to be analyzed for detection are equal size windows cut from the input image. The dimensions a×b are defined by the size of the structural unit, as selected by an operator.

The procedure to recognize the structural units involves three steps (see Figure 5): pre-processing, dimensionality reduction and classification.

The contrast in HRTEM images is a complex consequence of various experimental parameters like specimen thickness, defects in the microstructure, strain in the material, among others [Willi98]. Even pure crystalline samples may show variations in contrast due to problems in the specimen preparation.

In order to reduce the impact of the non-uniform contrast on the detector performance, histogram equalization is applied to each input image window w(x,y). Fig. 5 shows the effect on two input image windows having quite different contrast levels.

Effect of histogram equalization. Left - original images. Right - after pre-processing.
Figure 5.

2.1. DIMENSIONALITY REDUCTION

This approach initially takes the intensities of each pixel of an image window as its features. A window with n pixels can therefore be represented by a feature vector $\mathbf{x} = [x_1,..., x_n]$ obtained by concatenating the rows of the image window matrix. It is generally desirable to work with a small feature set, since it reduces the complexity of the classifier and eases its training. In this step the $n=a\times b$ pixel intensities of a window obtained after the pre-processing, are mapped onto a set of p features ($p<n$) by applying an extension of Principal Component Analysis (PCA) called, from this point on, MAXDIST [Mota00]. This procedure finds a subspace in which the average distance of the patterns to be detected to the other patterns present in the image is maximal.

Let $\mathbf{x}$ be a random vector representing the pattern of a window *not* belonging to class ω - the class to be detected. Let $\mathbb{m}$ be the centroid of class ω in the original feature space. Thus $(\mathbf{x} - \mathbb{m})$ represents the vectors linking the centroid of class ω to the patterns $\mathbf{x}$ ($\mathbf{x} \notin \omega$). Clearly $(\mathbf{x} - \mathbb{m})$ is also a random vector. Let $\mathbf{a} = [a_1, a_2, \ldots, a_n]$ be a unitary vector in the same space. The square of the projection of $(\mathbf{x} - \mathbb{m})$ over the vector $\mathbf{a}$ is given by:

$$\begin{aligned}\left[\mathbf{a}(\mathbf{x}-\boldsymbol{\mu})^T\right]^2 &= \left[(\mathbf{x}-\boldsymbol{\mu})\mathbf{a}^T\right]^2 \\ &= \mathbf{a}(\mathbf{x}-\boldsymbol{\mu})^T(\mathbf{x}-\boldsymbol{\mu})\mathbf{a}^T\end{aligned} \tag{2}$$

The expected value for this quantity will be:

$$\begin{aligned}&E\left[\mathbf{a}(\mathbf{x}-\boldsymbol{\mu})^T(\mathbf{x}-\boldsymbol{\mu})\mathbf{a}^T\right] = \\ &= \mathbf{a}\,E\left[(\mathbf{x}-\boldsymbol{\mu})^T(\mathbf{x}-\boldsymbol{\mu})\right]\mathbf{a}^T = \mathbf{a}\sum_d \mathbf{a}^T\end{aligned} \tag{3}$$

It can be noted that the matrix

$$\sum_d = E\left[(\mathbf{x}-\boldsymbol{\mu})^T(\mathbf{x}-\boldsymbol{\mu})\right] \tag{4}$$

has a definition similar to the usual covariance matrix, where the centroid of class ω takes the place of the population mean.

If $\sum_d$ is positive definite with eigenvalues $\lambda_1 \geq \lambda_2 \geq \ldots \geq \lambda_n > 0$ corresponding to eigenvectors $\mathbf{e}_1, \mathbf{e}_2, \ldots, \mathbf{e}_n$

it can be proven [Johns98] that

$$\max_{\mathbf{a}\neq\mathbf{0}} \mathbf{a}\sum_d \mathbf{a}^T = l_1 \quad (5)$$

and it is attained when $\mathbf{a} = \mathbf{e}_1$. Moreover

$$\max_{\mathbf{a}\perp\mathbf{e}_1,\mathbf{e}_2,\ldots,\mathbf{e}_p} \mathbf{a}\sum_d \mathbf{a}^T = l_{p+1} \quad (6)$$

which is attained for $\mathbf{a} = \mathbf{e}_{p+1}$.

The procedure described above identifies the *p*-dimensional subspace over which the average projection of the vectors going from the centroid of class ω to the patterns not belonging to it is a maximum. This subspace will be defined by the *p* eigenvalues of matrix $\sum_d$ with the highest eigenvalues - in other words, they will be the base of the wanted subspace.

The reader will probably recognize a close analogy between the development presented above and PCA. The MAXDIST approach maximizes the Euclidean distance of the patterns to the centroid of the class to be detected, whilst PCA is concerned with the Euclidean distance to the centroid of the entire population.

Following the same reasoning of PCA it can be shown that the average proportion (*P*) of the quadratic distance of the patterns not belonging to class ω to its centroid, expressed by the projection over the *p*-th eigenvector is given by:

$$P = \frac{l_p}{l_1 + l_2 + \cdots + l_n}, \quad (7)$$

If one takes the projections over the first *p* eigenvectors instead of all of them, an error in the computation of the quadratic distance to the centroid of the class to be detected will result. According to Eq. 7, its average is equal to

$$\hat{e} = \frac{l_{p+1} + \cdots + l_n}{l_1 + l_2 + \cdots + l_n}, \quad (8)$$

This error will be caused mainly by variations within the population that have a minor impact on the distance to the centroid of the class of interest. Therefore, this method reveals the features that most distinguish the patterns of interest from the others appearing in the image.

So the representation of a window in the new reduced feature space can be computed by:

$$\mathbf{y} = (\mathbf{x} - \boldsymbol{\mu})\mathbf{A}_p, \quad (9)$$

where the columns of matrix A_p are the *p* eigenvectors of $\sum_d$ with the largest eigenvalues.

Since m and $\sum_d$ are usually not available, estimates can be calculated by using the following equations:

$$\hat{\boldsymbol{\mu}} = \frac{1}{N_b}\sum_{\mathbf{x}\in ?} \mathbf{x} \quad (10)$$

$$\hat{\mathbf{S}}_d = \frac{1}{N_{\bar{b}}}\sum_{\mathbf{x}\notin ?} (\mathbf{x} - \hat{\boldsymbol{\mu}})^T (\mathbf{x} - \hat{\boldsymbol{\mu}}) \quad (11)$$

where N_b and $N_{\bar{b}}$ are respectively the number of training examples belonging and not belonging to class ω.

2.2. THE CLASSIFIER

A simple Euclidean Distance Classifier is used in this approach. For every pattern corresponding to a window cropped from the input image, its distance to the centroid of the class ω is computed and then compared to a given threshold *T*. If it is greater than or equal to the threshold the pattern is rejected - the window is considered as not enclosing a structural unit of the boundary. If the distance is less than *T*, the pattern is accepted - the window is assumed to have a structural unit of the boundary.

It is clear that the number of false detections - patterns erroneously assigned by the system as belonging to the class ω, also called false positives (fpos) - will increase by adopting higher values for the threshold *T*, whilst the number of false rejections - patterns erroneously assigned by the system as not belonging to the class ω, also called false negatives (fneg) - will decrease. So by varying the value of *T* the system will generate different pairs of values (fpos, fneg). By plotting these values a performance curve will be obtained, the so-called *Receiver Operating Characteristic (ROC)*. These curves will be presented in section 4 to compare the performance of this method with the performance of the standard cross-correlation technique.

3. BUILDING THE TRAINING SET

The experiments carried out to evaluate this approach have shown that a critical performance issue is the choice of the training set. Training the detector involves the computation of the sample average feature vector $\hat{\boldsymbol{\mu}}$, and the transformation matrix $\mathbf{A}_p$.

From a previous work [Dahme94] it is known that two types of structural units appear along the crystal boundary, as can be seen in the example of Figs.1 and 2. Structural units of each type appear exclusively along the crystal boundary. So the detector must be able to distinguish among three different pattern classes: *boundary type 1*, *boundary type 2* and *non-boundary*.

The *non-boundary* class corresponds to all a×b windows that can be cut from the input image and that do not fall in the other two classes. Clearly all the windows taken from the regions on both sides of the boundary containing the regular structure of a crystal must be assigned to the *non-boundary* class.

Furthermore, suppose that a window w_1 encloses a structural unit entirely. A window w_2, displaced a certain number of pixels relative to window w_1, may have a non-empty intersection with window w_1, but it will not cover the structural unit entirely. In order for the detector to be accurate, it must be able to assign window w_1 to the corresponding *boundary* class, and window w_2 to the *non-boundary* class. The training set must take all these cases properly into account.

The selection of patterns in the image for the *boundary* class may involve a substantial visual effort by the user. In order to minimize this inconvenience, the user is required to select just one pattern for each *boundary* class. This procedure allows a comparison to the cross-correlation method, where the user selects a single template as a reference.

Since a class is not expected to be properly represented in the training set by just one pattern, some additional patterns for the *boundary* classes are automatically provided. After the user has selected a window containing a structural unit for a boundary class, 8 additional image windows will be taken automatically, with center pixels belonging to the 8-neighborhood of the center pixel of the user selected window. This provides 9 different patterns for each *boundary* class, as shown in Fig 6.

The inclusion of these 8-neighbor image windows in the training set will make the classifier less restrictive concerning both boundary classes. However, it may increase the number of false detections. To compensate for this effect, the training procedure adds to the *non-boundary* class in the training set all image windows with center pixels lying at a given chessboard distance *d* from the center pixel of the user selected window. This is illustrated in Fig. 6c for *d*= 5.

To include patterns representing the regions on both sides of the boundary the user is asked to select one window in each of the crystal regions of the input image. Without further user intervention the training procedure will then take additional patterns consisting of windows regularly displaced relative to each other by *h* pixels down and to the right, covering an area with height and width approximately twice the dimensions of an individual window. Fig. 7 illustrates the procedure for *h*=3 pixels. In Fig. 7a the center pixel of the user-selected window is shown. Fig. 7b shows the center pixels of the windows automatically added by the training procedure. Fig. 7c shows the total area covered by these windows.

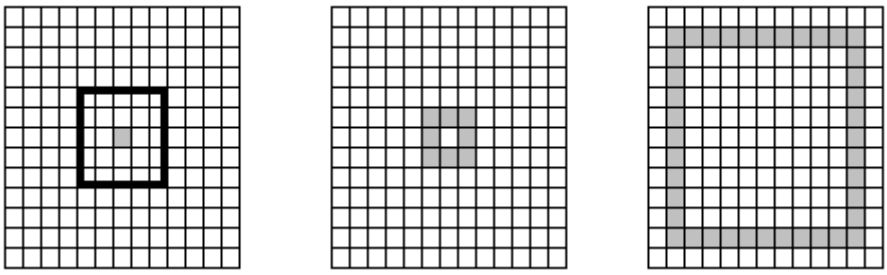

a b c

Training procedure: a) user selected window containing one pattern; b) central pixels of the automatically created windows containing other patterns added to the training set of the *boundary* class; c) central pixels of the automatically created windows containing patterns added to the training set of the *non-boundary* class.

Figure 6

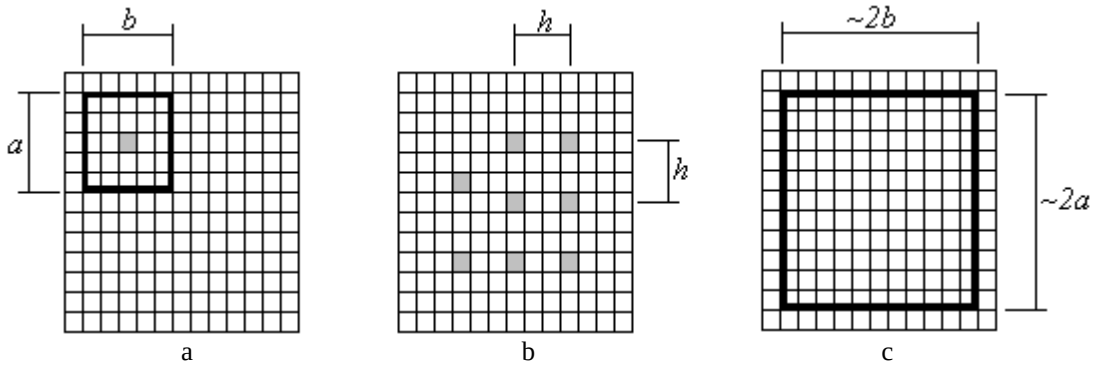

a b c

Training procedure using *k* patterns for each *boundary* class: a) window selected by the user; b) central pixels of the windows automatically added to the training set; c) area of the input image covered by windows associated with the training set of a *non-boundary* class

Figure 7

4. PERFORMANCE EVALUATION

The algorithm performance is dependent on the dimensionality reduction method, the number of components considered (*p*), and the threshold value used as decision boundary.

To compare the performance of the different methods, ROC curves were obtained varying the threshold value and determining the number of false positive and false negative detections. For PCA and MAXDIST, results were obtained for *p* varying between 5 and 50. The cross-correlation results were also plotted for comparison. Better results in the ROC graphs are represented by curves closer to the origin.

The training procedure described previously was used, whereby the most clearly visible structural unit of each *boundary* class was selected as the starting training example for these classes. The *non-boundary* examples were captured from the top and bottom crystals with *h*=5, and around the selected *boundary* examples for chessboard distance *d*=6.

The results for the TiO_2 boundary are presented in Fig. 8 for units of class *boundary 1* and Fig. 9 for class *boundary 2*. For clarity, only the ROC curves for 5 and 15 components appear on the graphs. The training set employed in this experiment contained 249 *non-boundary* examples, 153 cropped from the two crystal regions and 48 around each structural unit selected by the user, and the 9 *boundary* examples for each boundary class.

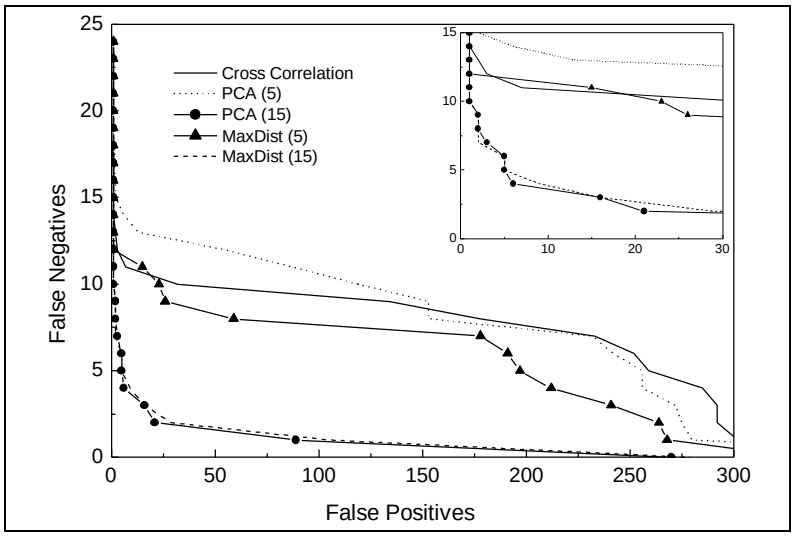

Comparison of the results provided by the Cross-correlation, PCA and MAXDIST methods in the detection of class *boundary 1* in the TiO_2 image.
Figure 8

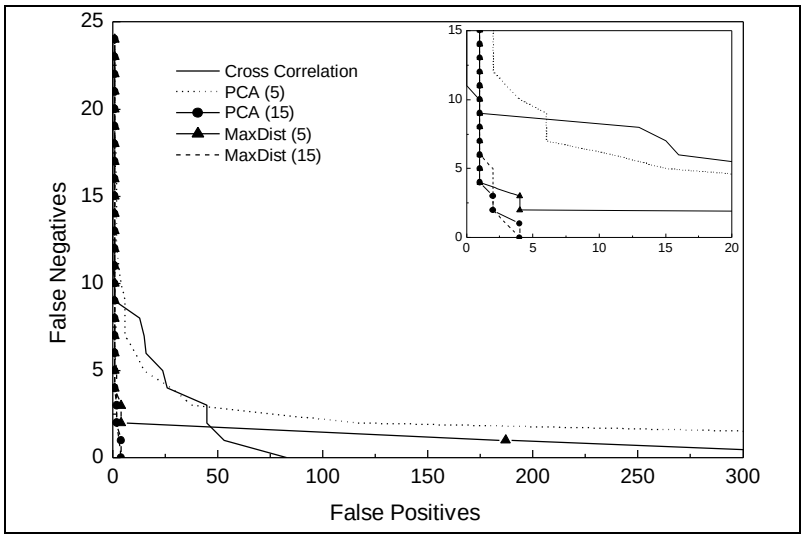

Comparison of the results provided by the Cross-correlation, PCA and MAXDIST methods in the detection of class *boundary 2* in the TiO_2 image.
Figure 9

A second HRTEM image, containing an Aluminum grain boundary, was analyzed to allow a more extensive test of the method. See Fig. 10.

The TiO_2 image has a simpler structure, as shown in Figure 4. Because of the periodic distribution of the structural units, it is relatively easy to establish the true number of units. In comparison, the Al boundary is much more complex. There is no periodic organization of the units and the image has more noise. The determination of the true number of units, to be used as a reference for the performance evaluation, required a substantial visual effort.

The results for the Al boundary are presented in Fig. 11. The training in this case comprised 182 *non-boundary* examples, 134 cropped from the two crystal regions and 48 around the structural unit selected by the user, and the 9 *boundary* examples for the boundary class.

The analysis of the graphs shows that both PCA and MAXDIST can produce better results than the cross-correlation method, depending on the number of components. This is the case for PCA with 15 components and MAXDIST with both 15 and 5 components. Cross-correlation is only superior to PCA with 5 components and for some threshold ranges.

Thus, the results confirm the initial expectation that both dimensionality reduction methods are able to detect the features that better distinguish the class to be detected from all others in the population. By disregarding features expressing the within-class variations PCA and MAXDIST allow for a better detection performance than can be reached by the cross-correlation method.

It can also be noted that the results obtained with PCA and MAXDIST with 15 components are essentially equivalent. For 5 components MAXDIST performs much better than PCA. These results along with the results from the experiments working with 5 to 50 components (and not shown in the graphs) consistently indicate that the MAXDIST method is more efficient than PCA in terms of dimensionality reduction for this kind of application.

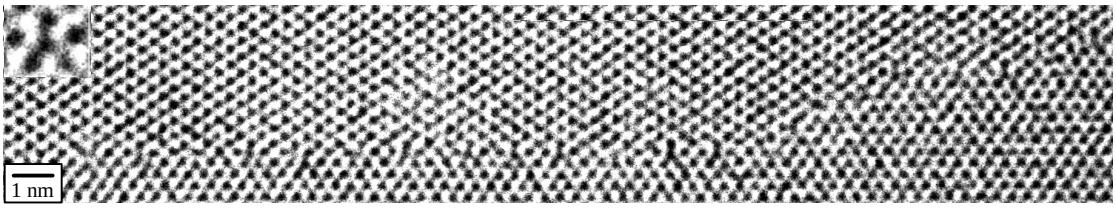

Aluminum grain boundary
Figure 10

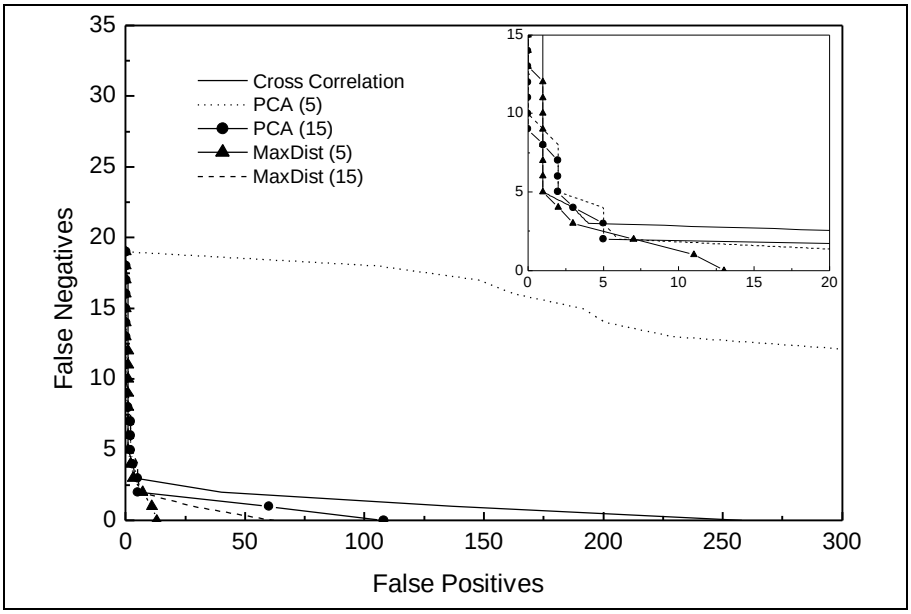

Comparison of the results provided by the Cross-correlation, PCA and MAXDIST methods in the Al image.
Figure 11

5. CONCLUSIONS

A new method (MAXDIST) for locating structural units in grain boundaries of materials imaged through HRTEM is proposed. Although the problem that motivated this research belongs to the area of Materials Science, the method proposed can be applied to any problem where a single pattern class is to be detected in a population enclosing a plurality of non well-defined classes.

The method consists of an extension of Principal Components Analysis, used for dimensionality reduction, followed by a conventional Distance Classifier.

Experiments on two different boundary images have shown that the proposed method attains a better tradeoff between false detections and false rejections than the conventional cross-correlation coefficient (CCC) approach. By using MAXDIST it was possible to represent an image window containing over a thousand pixels with as few as 5 attributes, and still perform better than the CCC method.

The dimensionality reduction afforded by MAXDIST has the potential to simplify the design and the training procedure of classifiers. This may allow the use of more sophisticated classifiers and eventually reach even better performance rates.

ACKNOWLEDGEMENTS

The authors wish to thank Dr. Ulrich Dahmen from NCEM/LBNL for making available the HRTEM images. Financial support by CNPq (Brazilian Research Council) and MCT (Brazilian Ministry of Science and Technology) through the RECOPE program, is also acknowledged.

REFERENCES

[Dahme94] - U.Dahmen, S.Paciornik, I.G.Solorzano and J.B.VanderSande – *HREM analysis of structure and defects in a S5 (210) grain boundary in Rutile* – Int. Sci. **2**, 127-138 (1994)

[Johns98] - R.A.Johnson, D.W. Wichern – *Applied Multivariate Statistical Analysis*, 4th Ed., Prentice Hall, (1998).

[Mota00] – G. L. A. Mota, *Detecção de Padrões em imagens bidimensionais: Estudo de casos*, Department of Electrical Engineering of the Catholic University of Rio de Janeiro, Msc. Dissertation (2000).

[Pacio96] - S.Paciornik, R.Kilaas, J.Turner and U.Dahmen – *A Pattern recognition technique for the analysis of grain boundary structure by HREM* – Ultramic. **62**, 15-27 (1996).

[Willi96] - D.B.Williams and C.B. Carter – *Transmission Electron Microscopy* – Plenum Press (1996).